International Journal of Mathematical Analysis and Optimization: Theory and Applications
Vol. 2020, No. 1, pp. 780 - 799

Coupled Effects of Surface Inclination and Magnetic Field on Free Convection Heat Transfer of Nanofluid over a Flat Plate in a Porous Medium in the Presence of Thermal Radiation

Sobamowo, M. G. [1*], Yinusa, A. A. [2], Waheed, M. A. [3]

[1*,2].Department of Mechanical Engineering, University of Lagos, Akoka, Lagos, Nigeria
[3]. Department of Mechanical Engineering, Federal University of Agriculture, Abeokuta, Ogun, Nigeria
*Corresponding author: gsobamowo@unilag.edu.ng

Article Info
Received: 29 June 2020 Revised: 12 August 2020
Accepted: 14 August 2020 Available online: 01 September 2020

Abstract

The present paper focuses on the impacts of stretching surface inclination, magnetic field and thermal radiation on natural convection heat transfer of nanofluids over a surface in a porous medium. The flow and heat transfer models are solved using multi-step differential transformation method. From the parametric study, the results show that the velocity of the nanofluid increases as the plate inclination increases while the temperature of the nanofluid decreases as the plate inclination increases. Also, the flow velocity of the fluid attains minimum value when the plate assumes horizontal position while it reaches maximum value when the plate is at vertical position. The velocity of the fluid decreases as the magnetic field parameter increases. However, the temperature gradient of the flow increases as the magnetic field parameter increases. The viscous and thermal boundary layers increase with the increase of thermal radiation parameter. The present study will help in the design of flow equipment in various industrial and engineering various applications.

Keywords and Phrases Free convection; flat plate inclination; Magnetic field; Nanofluid; Thermal radiation.
MSC2010: 74F10

1 Introduction

Flow over flat surfaces are dominated in various applications such as solar extrusion, coating, aeronautics, solar energy, melt spinning, cooling of metallic plates, glass-fiber production, food processing, mechanical forming, reactor fluidization, foodstuff processing, drawing of a polymer sheet, aerodynamic, cooling of gas turbine rotor blades, continuous casting, rolling, heat treatment, tinning of copper wires, etc. In these applications, the fluid flow and heat transfer analyses are very important as the quality of products in the processes depends considerably on the flow and heat transfer characteristics of thin liquid films over the stretching sheets. A common application of fluid flow over flat surface in renewable energy applications is the fluid flow over a photovoltaic solar panel as shown in Fig. 1. Consequently, flow and heat transfer of fluids over flat surfaces has been a subject of study over the past decades [1]-[11]. Also, in a recent study, Na and Habib [12] adopted parameter differentiation method to examine the free convection boundary layer flow problem over a vertical surface. Merkin [13] submitted the similarity solutions for natural convection on a vertical plate while Merkin and Pop [14] used finitedifference method to have insight into the conjugate free convection problem of boundary-layer flow over a vertical plate. Ali et al. [15] presented a numerical investigation of free convective boundary layer in a viscous fluid while Motsa et al. [16] utilized homotopy analysis method to solve the flow problem but with the inclusion of mass transfer. Also, spectral local linearization approach was used by the same author [17] to the problem while Ghotbi et al. [18] developed analytical solutions to the problem using homotopy analysis method. The previous studies on the problem under investigation are based on the flow of viscous fluid over a vertical surface without considering the effects of plate inclination on the flow behaviour. To the best of the author's knowledge, a study on the coupled effects of plate inclination, magnetic field and thermal radiation on the free convection boundary-layer flow and heat transfer of nanofluids over a vertical plate using multi-step differential transformation method has not been carried out in an open literature. Therefore, the present study provides insights on the coupled effect of stretching plate inclination, magnetic field and thermal radiation on natural convection heat transfer of nanofluids over a surface with thermal radiation using multi-step differential transformation method. The developed analytical solutions are used for parametric studies and the results are presented and discussed.

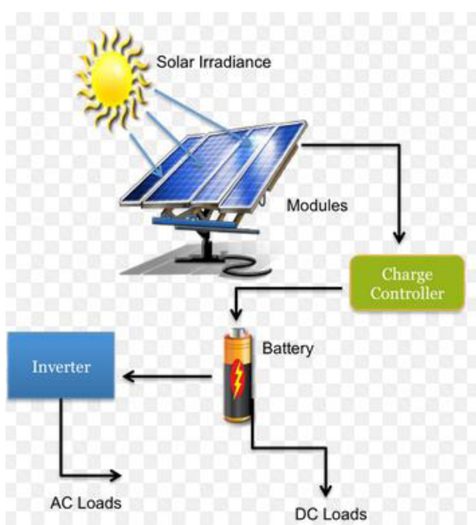

Figure 1: Power generation through an inclined photovoltaic solar panel

International Journal of Mathematical Analysis and Optimization: Theory and Applications
Vol. 2020, No. 1, pp. 780 - 799

2 Problem Formulation and Mathematical analysis

Consider a laminar natural convection flow of an incompressible electrically conducting nanofluid past a plate embedded in a porous medium which is inclined to the horizontal with an acute angle γ measured in the anticlockwise direction and situated in an otherwise quiescent ambient fluid at temperature T_w as shown in Fig. 2. A transverse magnetic field of strength B is applied normal to the inclined plate as shown in the figure.

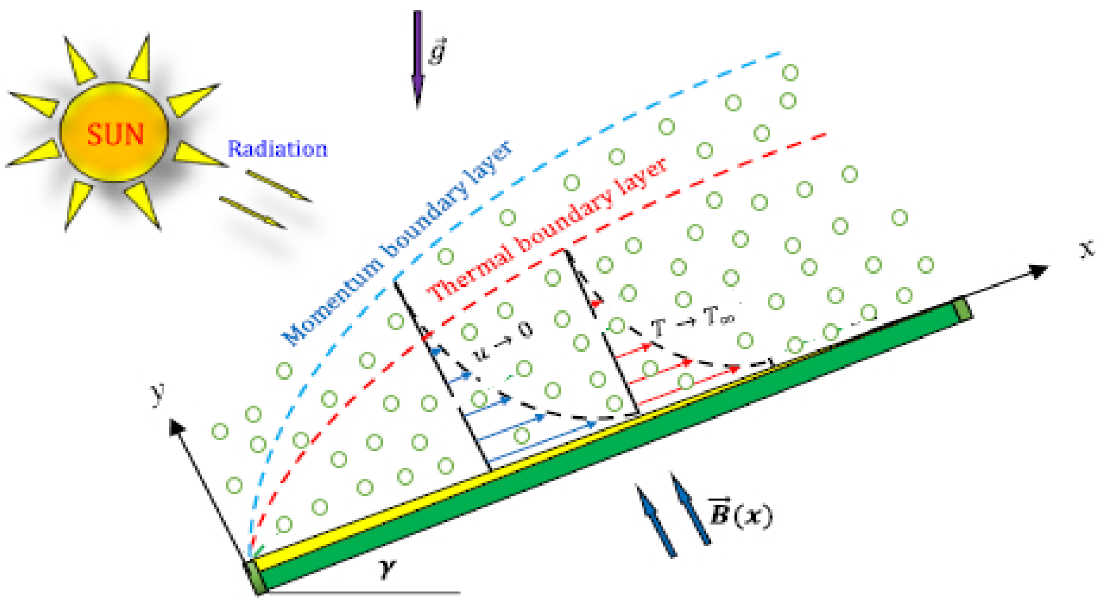

Figure 2: Velocity and temperature profiles in free convection flow of nanofluid over an inclined plate embedded in a porous medium

For the steady, incompressible, two-dimensional laminar flow, the equations for continuity, momentum and energy are given as

$$\frac{\partial u}{\partial x} + \frac{\partial v}{\partial y} = 0 \tag{2.1}$$

$$\rho_{nf}\left(u\frac{\partial u}{\partial x} + v\frac{\partial u}{\partial y}\right) = \mu_{nf}\frac{\partial^2 u}{\partial y^2} + g\,(\rho\beta)_{nf}\,(T - T_\infty)\,sin\gamma - \sigma B_o^2 u - \frac{\mu_{nf} u}{K_p} \tag{2.2}$$

$$(\rho c_p)_{nf}\left(u\frac{\partial T}{\partial x} + v\frac{\partial T}{\partial y}\right) = k_{nf}\frac{\partial^2 T}{\partial y^2} - \frac{\partial q_r}{\partial y} \tag{2.3}$$

Using Rosseland's approximation, the radiation term at the RHS of Eq. (2.3) can be expressed as

$$\frac{\partial q_r}{\partial y} = -\frac{4\sigma}{3K}\frac{\partial T^4}{\partial y} \cong -\frac{16\sigma_{rad}T_s^3}{3K}\frac{\partial^2 T}{\partial y^2} \tag{2.4}$$

Therefore, the energy equation in Eq. (2.3) becomes

$$(\rho c_p)_{nf}\left(u\frac{\partial T}{\partial x} + v\frac{\partial T}{\partial y}\right) = \left(k_{nf} + \frac{16\sigma_{rad}T_s^3}{3K}\right)\frac{\partial^2 T}{\partial y^2} \tag{2.5}$$

International Journal of Mathematical Analysis and Optimization: Theory and Applications
Vol. 2020, No. 1, pp. 780 - 799

Under no slip conditions, the appropriate boundary conditions are given as

$$\begin{gathered} u=0, \quad v=0, \quad T=T_s \quad at \quad y=0 \\ u=0, \quad T=T_w, \quad at\; y\rightarrow\infty \end{gathered} \tag{2.6}$$

The various physical and thermal properties of the nanofluid are presented as follows:

$$\begin{aligned} \rho_{nf} &= \rho_f(1-\phi)+\rho_s\phi \\ (\rho c_p)_{nf} &= (\rho c_p)_f(1- \ phi)+(\rho c_p)_s\phi \\ (\rho\beta)_{nf} &= (\rho\beta)_f(1-\phi)+(\rho\beta)_s\phi \end{aligned} \tag{2.7}$$

$$\mu_{nf}=\frac{\mu_f}{(1-\phi)^{2.5}} \tag{2.8}$$

$$k_{nf}=k_f\left[\frac{k_s+2k_f-2\phi(k_f-k_s)}{k_s+2k_f+\phi(k_f-k_s)}\right] \tag{2.9}$$

$$\sigma_{nf}=\sigma_f\left[1+\frac{3\left\{\frac{\sigma_s}{\sigma_f}-1\right\}\phi}{\left\{\frac{\sigma_s}{\sigma_f}+2\right\}\phi-\left\{\frac{\sigma_s}{\sigma_f}-1\right\}\phi}\right], \tag{2.10}$$

From Eq. (2.1), (2.2) and (2.3), introducing a stream function, $\psi(x,y)$ such that

$$u=\frac{\partial\psi}{\partial y},\quad v=-\frac{\partial\psi}{\partial x}, \tag{2.11}$$

and using the similarity and dimensionless variables as

$$\begin{gathered} \eta=\left[\frac{\rho_{nf}^2\left(g\beta_{nf}(T_w-T_\infty)\right)}{4\mu_{nf}^2x}\right]^{\frac{1}{4}}y,\quad \psi=\frac{4\mu_{nf}}{\rho_{nf}}\left[\frac{\rho_{nf}^2\left(g\beta_{nf}(T_w-T_\infty)\right)x^3}{4\mu_{nf}^2}\right]^{1/4}f(\eta), \\ Gr=\frac{g\beta_{nf}v_{nf}(T_w-T_\infty)}{u_\infty^3},\quad \theta=\frac{T-T_\infty}{T_w-T_\infty},\quad Pr=\frac{\mu_{nf}c_p}{k_{nf}} \\ R=\frac{4\sigma_{rad}T_\infty^3}{3kK},\quad Ha^2=\frac{\sigma_{nf}B_0^2v_{nf}}{\rho_{nf}u_\infty^2Gr}, \\ Da=\frac{u_\infty^2K_pGr}{v_{nf}^2} \end{gathered} \tag{2.12}$$

fully coupled third and second orders ordinary differential equations are derived as

$$f'''(\eta)+(1-\phi)^{2.5}\left\{\begin{array}{l}\left[(1-\phi)+\phi\left(\frac{\rho_s}{\rho_f}\right)\right]\left(3f(\eta)f''(\eta)-2\left(f'(\eta)\right)^2\right)\\ +\left[(1-\phi)+\phi\left[(\rho\beta)_s\Big/(\rho\beta)_f\right]\right]\theta(\eta)\,sin\gamma\end{array}\right\} -\left(Ha^2+\frac{1}{Da}\right)f(\eta)=0 \tag{2.13}$$

$$\left(1+\frac{4}{3}R\right)\theta''+3\left[\frac{1}{\left[(1-\phi)+\phi\left[(\rho C_p)_s\Big/(\rho C_p)_f\right]\right]}\left[\frac{k_s+2k_f-2\phi(k_f-k_s)}{k_s+2k_f+\phi(k_f-k_s)}\right]\right]Prf\theta'=0 \tag{2.14}$$

and the boundary conditions as

$$\begin{gathered} f=0,\quad f'=0,\quad \theta=1,\quad when\;\eta=0 \\ f'=0,\quad \theta=0,\quad when\;\eta=\infty \end{gathered} \tag{2.15}$$

International Journal of Mathematical Analysis and Optimization: Theory and Applications
Vol. 2020, No. 1, pp. 780 - 799

3 Basic Concepts of Multi-Step differential transform method

The basic concept, the definitions of classical differential transformation method and multi-step differential transformation method can be found in our previous publication, Sobamowo and Yinusa [19].
With the aid of the operational properties of the classical differential transformation method in [19], the differential transformations of the flow equation in Eq. (2.13) is given as

$$(p+1)(p+2)(p+3)F(p+3) + (1-\phi)^{5/2}\left\{\begin{array}{l}\alpha_1\left[\begin{array}{l}3\sum_{l=0}^{p}(p-l+1)(p-l+2)F(l)F(p-l+2)\\ -2\sum_{l=0}^{p}(l+1)(p-l+1)F(l+1)F(p-l+1)\end{array}\right]\\ +\alpha_2\Theta(p)\sin\gamma-\left(Ha^2+Da^{-1}\right)F(p)\end{array}\right\}=0 \tag{3.1}$$

Also, for Eq. (2.14),

$$(p+1)(p+2)\Theta(p+2)+\left\{3\alpha_3 Pr\sum_{l=0}^{p}(l+1)\Theta(l+1)F(p-l)\right\}=0 \tag{3.2}$$

We can write Eq. (3.1) as

$$F(p+3)=\frac{(1-\phi)^{5/2}}{(p+1)(p+2)(p+3)}\left\{\begin{array}{l}\alpha_1\left[\begin{array}{l}2\sum_{l=0}^{p}(l+1)(p-l+1)F(l+1)F(p-l+1)\\ -3\sum_{l=0}^{p}(p-l+1)(p-l+2)F(l)F(p-l+2)\end{array}\right]\\ -\alpha_2\Theta(p)\,sin\gamma+\left(Ha^2+Da^{-1}\right)F(p)\end{array}\right\} \tag{3.3}$$

And Eq. (3.2) as

$$\Theta(p+2)=\frac{-3\alpha_3 Pr}{(p+1)(p+2)}\left\{\sum_{l=0}^{p}(l+1)\Theta(l+1)F(p-l)\right\} \tag{3.4}$$

where

$$\begin{aligned}\alpha_1&=(1-\phi)+\phi\left(\frac{\rho_s}{\rho_f}\right)\\ \alpha_2&=\left[(1-\phi)+\phi\left[(\rho\beta)_s\big/(\rho\beta)_f\right]\right]\\ \alpha_3&=\left[\frac{1}{\left[(1-\phi)+\phi\left[(\rho C_p)_s/(\rho C_p)_f\right]\right]}\left[\frac{k_s+(m-1)k_f-(m-1)\phi(k_f-k_s)}{k_s+(m-1)k_f+\phi(k_f-k_s)}\right]\right]\end{aligned}$$

The recursive relations for the boundary conditions in Eq. (2.15) are

$$\begin{array}{l}F(p)=0\Rightarrow F(0)=0,\quad (p+1)F(p+1)=0\quad\Rightarrow F(1)=0,\\ \theta(p)=1\quad\Rightarrow\theta(0)=1,\quad F(2)=a,\quad\theta(1)=b,\end{array} \tag{3.5}$$

where a and b are unknown constants which will be found later.

It should be noted that the transformations which included "a" and"b" are established from values of$f''(0)=a$ and $\theta'(0)=b$.

Therefore, from Eq. (3.5), we have the following boundary conditions in differential transform domain

$$F[0]=0,\quad F[1]=0,\quad\theta[0]=1,\quad F[2]=a,\quad\theta[1]=b \tag{3.6}$$

Using p=*0, 1, 2, 3, 4, 5, 6, 7...* in the above recursive relations in Eq. (3.3), the following equations are obtained

$$F[3]=-\frac{1}{6}(1-\phi)^{5/2}\alpha_2 sin\gamma$$

IJMAO

International Journal of Mathematical Analysis and Optimization: Theory and Applications
Vol. 2020, No. 1, pp. 780 - 799

$$F[4]=-\frac{1}{24}(1-\phi)^{5/2}\,b\,\alpha_2 sin\gamma$$

$$F[5]=\frac{a\left(2a(1-\phi)^{5/2}\alpha_1 Da+Ha^2Da+1\right)}{60Da}$$

$$F[6]=-\frac{\left(DaHa^2+1\right)(1-\phi)^{5/2}\alpha_2 sin\gamma}{720Da}$$

$$F[7]=-\frac{(1-\phi)^{5/2}\alpha_2 bsin\gamma\left(\begin{array}{l}-40Da(1-\phi)^{5/2}Rda\alpha_1-30(1-\phi)^{5/2}\alpha_1 aDa\\+4DaHa^2Rd-18DaPra\alpha_3+3DaHa^2+4Rd+3\end{array}\right)}{(15120+20160Rd)\,Da}$$

$$F[8]=\frac{1}{(120960+161280Rd)Da^2}\left(\begin{array}{l}6a+8Da^2Ha^4Rda+16DaHa^2Rda-144(1-\phi)^{5/2}\alpha_1 a^2Da\\+312Da^2a^3\phi^5{\alpha_1}^2-1560Da^2a^3\phi^4{\alpha_1}^2+3120Da^2a^3\phi^3{\alpha_1}^2\\-3120Da^2a^3\phi^2{\alpha_1}^2+1560Da^2a^3\phi{\alpha_1}^2-416Da^2Rda^3{\alpha_1}^2\\-192Da^2Ha^2(1-\phi)^{5/2}Rda^2\alpha_1-15Da^2(1-\phi)^{5/2}b(sin\gamma)^2\alpha_1{\alpha_2}^2\\-9Da^2Prb(sin\gamma)^2{\alpha_2}^2\alpha_3+100Da^2(1-\phi)^{5/2}Rdb(sin\gamma)^2\phi\alpha_1{\alpha_2}^2\\-200Da^2(1-\phi)^{5/2}Rdb(sin\gamma)^2\phi^2\alpha_1{\alpha_2}^2\\-100Da^2(1-\phi)^{5/2}Rdb(sin\gamma)^2\phi^4\alpha_1{\alpha_2}^2\\+200Da^2(1-\phi)^{5/2}Rdb(sin\gamma)^2\phi^3\alpha_1{\alpha_2}^2\\+20Da^2(1-\phi)^{5/2}Rdb(sin\gamma)^2\phi^5\alpha_1{\alpha_2}^2-192Da(1-\phi)^{5/2}Rda^2\alpha_1\\-144Da^2Ha^2(1-\phi)^{5/2}a^2\alpha_1-4160Da^2Rda^3\phi^2{\alpha_1}^2\\+2080Da^2Rda^3\phi{\alpha_1}^2+4160Da^2Rda^3\phi^3{\alpha_1}^2+416Da^2Rda^3\phi^5{\alpha_1}^2\\-2080Da^2Rda^3\phi^4{\alpha_1}^2+8Rda+12DaHa^2a-312Da^2a^3{\alpha_1}^2\\+6Da^2Ha^4a-20Da^2(1-\phi)^{5/2}Rdb(sin\gamma)^2\alpha_1{\alpha_2}^2\\+75Da^2(1-\phi)^{5/2}b(sin\gamma)^2\phi\alpha_1{\alpha_2}^2\\+150Da^2(1-\phi)^{5/2}b(sin\gamma)^2\phi^3\alpha_1{\alpha_2}^2\\-150Da^2(1-\phi)^{5/2}b(sin\gamma)^2\phi^2\alpha_1{\alpha_2}^2\\+15Da^2(1-\phi)^{5/2}b(sin\gamma)^2\phi^5\alpha_1{\alpha_2}^2\\-75Da^2(1-\phi)^{5/2}b(sin\gamma)^2\phi^4\alpha_1{\alpha_2}^2+9Da^2Prb(sin\gamma)^2\phi^5{\alpha_2}^2\alpha_3\\-45Da^2Prb(sin\gamma)^2\phi^4{\alpha_2}^2\alpha_3+90Da^2Prb(sin\gamma)^2\phi^3{\alpha_2}^2\alpha_3\\-90Da^2Prb(sin\gamma)^2\phi^2{\alpha_2}^2\alpha_3+45Da^2Prb(sin\gamma)^2\phi{\alpha_2}^2\alpha_3\end{array}\right)$$

$$F[9]=-\frac{(1-\phi)^{5/2}\alpha_2 sin\gamma}{(1088640+1451520Rd)Da^2}\left(\begin{array}{l}3-252(1-\phi)^{5/2}\alpha_1 aDa+216Da^2a^2\phi^5{\alpha_1}^2-1080Da^2a^2\phi^4{\alpha_1}^2\\+2160Da^2a^2\phi^3{\alpha_1}^2-2160Da^2a^2\phi^2{\alpha_1}^2+1080Da^2a^2\phi{\alpha_1}^2\\-288Da^2Rda^2{\alpha_1}^2-15Da^2b^2\phi^5\alpha_1\alpha_2 sin\gamma+75Da^2b^2\phi^4\alpha_1\alpha_2 sin\gamma\\-150Da^2b^2\phi^3\alpha_1\alpha_2 sin\gamma+150Da^2b^2\phi^2\alpha_1\alpha_2 sin\gamma+20Da^2Rdb^2\alpha_1\alpha_2 sin\gamma\\-75Da^2b^2\phi\alpha_1\alpha_2 sin\gamma-336Da^2Ha^2(1-\phi)^{5/2}Rda\alpha_1+8DaHa^2Rd\\+200Da^2Rdb^2\phi^2\alpha_1\alpha_2 sin\gamma+100Da^2Rdb^2\phi^4\alpha_1\alpha_2 sin\gamma\\-1440Da^2Rda^2\phi^4{\alpha_1}^2-200Da^2Rdb^2\phi^3\alpha_1\alpha_2 sin\gamma\\+9Da^2(1-\phi)^{5/2}Prb^2\alpha_2\alpha_3 sin\gamma-20Da^2Rdb^2\phi^5\alpha_1\alpha_2 sin\gamma\\-100Da^2Rdb^2\phi\alpha_1\alpha_2 sin\gamma-336Da(1-\phi)^{5/2}Rda\alpha_1\\+288Da^2Rda^2\phi^5{\alpha_1}^2+15Da^2b^2\alpha_1\alpha_2 sin\gamma-252Da^2Ha^2(1-\phi)^{5/2}a\alpha_1\\-2880Da^2Rda^2\phi^2{\alpha_1}^2+1440Da^2Rda^2\phi{\alpha_1}^2+2880Da^2Rda^2\phi^3{\alpha_1}^2\\+6Ha^2Da+3Da^2Ha^4+4Da^2Ha^4Rd-216Da^2a^2{\alpha_1}^2+4Rd\end{array}\right)$$

$$F[10]=-\frac{(1-\phi)^{5/2}\alpha_2 sin\gamma}{3628800(3+4Rd)^2Da^2}\left(\begin{array}{l}-77760Da^2Rda^2b\phi{\alpha_1}^2+9b+5832Da^2a^2b{\alpha_1}^2+16Da^2Ha^4Rd^2b\\+24Da^2Ha^4Rdb+32DaHa^2Rd^2b+48DaHa^2Rdb+378Da\alpha_1\alpha_2sin\gamma\\-378Da^2Ha^2\phi^5\alpha_1\alpha_2sin\gamma+1890Da^2Ha^2\phi^4\alpha_1\alpha_2sin\gamma\\-672DaRd^2\phi^5\alpha_1\alpha_2sin\gamma-3780Da^2Ha^2\phi^3\alpha_1\alpha_2sin\gamma\\+3360DaRd^2\phi^4\alpha_1\alpha_2sin\gamma-1008DaRd\phi^5\alpha_1\alpha_2sin\gamma\\+672Da^2Ha^2Rd^2\alpha_1\alpha_2sin\gamma-6720DaRd^2\phi^3\alpha_1\alpha_2sin\gamma\\+5040DaRd\phi^4\alpha_1\alpha_2sin\gamma-10368Da^2Rd^2a^2b\phi^5{\alpha_1}^2\\+51840Da^2Rd^2a^2b\phi^4{\alpha_1}^2-15552Da^2Rda^2b\phi^5{\alpha_1}^2\\-103680Da^2Rd^2a^2b\phi^3{\alpha_1}^2+77760Da^2Rda^2b\phi^4{\alpha_1}^2\\+103680Da^2Rd^2a^2b\phi^2{\alpha_1}^2-155520Da^2Rda^2b\phi^3{\alpha_1}^2\\-51840Da^2Rd^2a^2b\phi{\alpha_1}^2+155520Da^2Rda^2b\phi^2{\alpha_1}^2\\+5328Da^2\left(1-\phi\right)^{5/2}PrRda^2b\alpha_1\alpha_3+3780Da\phi^2\alpha_1\alpha_2sin\gamma\\+672DaRd^2\alpha_1\alpha_2sin\gamma+378Da^2Ha^2\alpha_1\alpha_2sin\gamma\\+3360Da^2Ha^2Rd^2\phi^4\alpha_1\alpha_2sin\gamma-3780Da\phi^3\alpha_1\alpha_2sin\gamma\\+1890Da\phi^4\alpha_1\alpha_2sin\gamma+3240Da^2Pra^2b{\alpha_3}^2-378Da\phi^5\alpha_1\alpha_2sin\gamma\\+10080Da^2Ha^2Rd\phi^2\alpha_1\alpha_2sin\gamma-3360Da^2Ha^2Rd^2\phi\alpha_1\alpha_2sin\gamma\\-10080Da^2Ha^2Rd\phi^3\alpha_1\alpha_2sin\gamma+6720Da^2Ha^2Rd^2\phi^2\alpha_1\alpha_2sin\gamma\\+5040Da^2Ha^2Rdsin\gamma\phi^4\alpha_1\alpha_2-6720Da^2Ha^2Rd^2sin\gamma\phi^3\alpha_1\alpha_2\\-1008Da^2Ha^2Rd\phi^5\alpha_1\alpha_2sin\gamma-3408Da\left(1-\phi\right)^{5/2}Rdab\alpha_1\\+3780Da^2Ha^2\phi^2\alpha_1\alpha_2sin\gamma-2272Da\left(1-\phi\right)^{5/2}Rd^2ab\alpha_1\\-1278Da^2Ha^2\left(1-\phi\right)^{5/2}ab\alpha_1-5040DaRd\phi\alpha_1\alpha_2sin\gamma\\-144DaPrRdab\alpha_3+10080DaRd\phi^2\alpha_1\alpha_2sin\gamma-3360DaRd^2\phi\alpha_1\alpha_2sin\gamma\\-10080DaRd\phi^3\alpha_1\alpha_2sin\gamma+6720DaRd^2\phi^2\alpha_1\alpha_2sin\gamma-\\1890Da^2Ha^2\phi\alpha_1\alpha_2sin\gamma+1008Da^2Ha^2Rd\alpha_1\alpha_2sin\gamma\\-672Da^2Ha^2Rd^2\phi^5\alpha_1\alpha_2sin\gamma-108Da^2Ha^2Prab\alpha_3\\+9Da^2Ha^4b+18DaHa^2b-1278Da\left(1-\phi\right)^{5/2}ab\alpha_1-108DaPrab\alpha_3\\+1008DaRd\alpha_1\alpha_2sin\gamma-1890Da\phi\alpha_1\alpha_2sin\gamma+58320Da^2a^2b\phi^2{\alpha_1}^2\\-29160Da^2a^2b\phi{\alpha_1}^2+29160Da^2a^2b\phi^4{\alpha_1}^2-58320Da^2a^2b\phi^3{\alpha_1}^2\\-5832Da^2a^2b\phi^5{\alpha_1}^2+10368Da^2Rd^2a^2b{\alpha_1}^2+15552Da^2Rda^2b{\alpha_1}^2\\+16Rd^2b+24Rdb-5040Da^2Ha^2Rd\phi\alpha_1\alpha_2sin\gamma-144Da^2Ha^2PrRdab\alpha_3\\+3996Da^2\left(1-\phi\right)^{5/2}Pra^2b\alpha_1\alpha_3-3408Da^2Ha^2\left(1-\phi\right)^{5/2}Rdab\alpha_1\\-2272Da^2Ha^2\left(1-\phi\right)^{5/2}Rd^2ab\alpha_1\end{array}\right)$$

In the same manner, the expressions for *F [11], F[12], F[13], F[14], F[15]* are found but they are too large to be included in this paper.
Also, taking *p=0, 1, 2, 3...* in the above recursive relations in Eq. (3.1), the solutions are derived as

$$\Theta[2]=0$$

$$\Theta[3]=0$$

$$\Theta[4]=-\frac{3}{4}\left(\frac{\alpha_3Pra\,b}{3+4Rd}\right)$$

$$\Theta[5]=\frac{3\alpha_3Pr\left(1-\phi\right)^{5/2}b\,\alpha_2sin\gamma}{120+160Rd}$$

$$\Theta[6]=\frac{\alpha_3Prb^2\left(1-\phi\right)^{5/2}\alpha_2sin\gamma}{240+320Rd}$$

$$\Theta[7]=-\frac{\alpha_3Prba\left(\begin{array}{c}3+8Da\left(1-\phi\right)^{5/2}Rda\alpha_1+6\left(1-\phi\right)^{5/2}\alpha_1aDa\\+4DaHa^2Rd-180DaPra\alpha_3+3DaHa^2+4Rd\end{array}\right)}{280\left(3+4Rd\right)^2Da}$$

$$\Theta[8]=\frac{\alpha_3 Pr\left(1-\phi\right)^{5/2} b\,\alpha_2\left(4DaHa^2Rd-630DaPra\alpha_3+3DaHa^2+4Rd+3\right)sin\gamma}{4480\left(3+4Rd\right)^2 Da}$$

$$\Theta[9]=\frac{\alpha_3 Prb\alpha_2 sin\gamma}{40320(3+4Rd)^2 Da}\left(\begin{array}{l} 4DaHa^2\left(1-\phi\right)^{5/2}Rdb-1026\alpha_3 Prba\left(1-\phi\right)^{5/2}Da- \\ 315DaPr\phi^5\alpha_2\alpha_3 sin\gamma+40DaRdab\phi^5\alpha_1+3DaHa^2\left(1-\phi\right)^{5/2}b+ \\ 1575DaPr\phi^4\alpha_2\alpha_3 sin\gamma-200DaRdab\phi^4\alpha_1+30Daab\phi^5\alpha_1+ \\ 150Daab\phi\alpha_1-30Daab\alpha_1-3150DaPr\phi^3\alpha_2\alpha_3 sin\gamma+400DaRdab\phi^3\alpha_1 \\ -150Daab\phi^4\alpha_1+3150DaPr\phi^2\alpha_2\alpha_3 sin\gamma-400DaRdab\phi^2\alpha_1 \\ +300Daab\phi^3\alpha_1+4\left(1-\phi\right)^{5/2}Rdb-1575DaPr\phi\alpha_2\alpha_3 sin\gamma \\ +200DaRdab\phi\alpha_1-300Daab\phi^2\alpha_1+3b\left(1-\phi\right)^{5/2} \\ +315\alpha_3 Pr\alpha_2 Dasin\gamma-40DaRdab\alpha_1 \end{array}\right)$$

International Journal of Mathematical Analysis and Optimization: Theory and Applications
Vol. 2020, No. 1, pp. 780 - 799

$$\Theta[10] = -\frac{\alpha_3 Prb}{403200(3+4Rd)^3 Da^2}\left(\begin{array}{l}
-1152Da^2Ha^2(1-\phi)^{5/2}Rda^2\alpha_1 - 450Da^2(1-\phi)^{5/2}b(sin\gamma)^2\phi^2\alpha_1{\alpha_2}^2\\
+18a - 9072\alpha_3Pra^2Da + 48Da^2Ha^4Rda + 96DaHa^2Rda-\\
432(1-\phi)^{5/2}\alpha_1a^2Da + 936Da^2a^3\phi^5{\alpha_1}^2 - 4680Da^2a^3\phi^4{\alpha_1}^2+\\
9360Da^2a^3\phi^3{\alpha_1}^2 - 9360Da^2a^3\phi^2{\alpha_1}^2 + 4680Da^2a^3\phi{\alpha_1}^2\\
-45Da^2(1-\phi)^{5/2}b(sin\gamma)^2\alpha_1{\alpha_2}^2 - 12096Da^2Ha^2PrRda^2\alpha_3\\
-18144Da^2(1-\phi)^{5/2}Pra^3\alpha_1\alpha_3 - 768Da^2Ha^2(1-\phi)^{5/2}Rd^2a^2\alpha_1\\
-12096DaPrRda^2\alpha_3 - 9072Da^2Ha^2Pra^2\alpha_3\\
+450Da^2(1-\phi)^{5/2}b(sin\gamma)^2\phi^3\alpha_1{\alpha_2}^2\\
-225Da^2(1-\phi)^{5/2}b(sin\gamma)^2\phi^4\alpha_1{\alpha_2}^2 + 45Da^2(1-\phi)^{5/2}b(sin\gamma)^2\phi^5\alpha_1{\alpha_2}^2\\
+3429Da^2Prb(sin\gamma)^2\phi^5{\alpha_2}^2\alpha_3\\
+34290Da^2Prb(sin\gamma)^2\phi^3{\alpha_2}^2\alpha_3 - 34290Da^2Prb(sin\gamma)^2\phi^2{\alpha_2}^2\alpha_3\\
-80Da^2(1-\phi)^{5/2}Rd^2b(sin\gamma)^2\alpha_1{\alpha_2}^2 - 4572Da^2PrRdb(sin\gamma)^2{\alpha_2}^2\alpha_3\\
-17145Da^2Prb(sin\gamma)^2\phi^4{\alpha_2}^2\alpha_3 - 120Da^2(1-\phi)^{5/2}Rdb(sin\gamma)^2\alpha_1{\alpha_2}^2\\
-24192Da^2(1-\phi)^{5/2}PrRda^3\alpha_1\alpha_3 + 225Da^2(1-\phi)^{5/2}b(sin\gamma)^2\phi\alpha_1{\alpha_2}^2\\
+600Da^2(1-\phi)^{5/2}Rdb(sin\gamma)^2\phi\alpha_1{\alpha_2}^2\\
-1200Da^2(1-\phi)^{5/2}Rdb(sin\gamma)^2\phi^2\alpha_1{\alpha_2}^2\\
+1200Da^2(1-\phi)^{5/2}Rdb(sin\gamma)^2\phi^3\alpha_1{\alpha_2}^2\\
-600Da^2(1-\phi)^{5/2}Rdb(sin\gamma)^2\phi^4\alpha_1{\alpha_2}^2\\
+120Da^2(1-\phi)^{5/2}Rdb(sin\gamma)^2\phi^5\alpha_1{\alpha_2}^2 + 32Rd^2a + 18Da^2Ha^4a\\
-1152Da(1-\phi)^{5/2}Rda^2\alpha_1 - 432Da^2Ha^2(1-\phi)^{5/2}a^2\alpha_1\\
+12480Da^2Rda^3\phi{\alpha_1}^2 - 936Da^2a^3{\alpha_1}^2 - 3429Da^2Prb(sin\gamma)^2{\alpha_2}^2\alpha_3\\
+17145Da^2Prb(sin\gamma)^2\phi{\alpha_2}^2\alpha_3 + 400Da^2(1-\phi)^{5/2}Rd^2b(sin\gamma)^2\phi\alpha_1{\alpha_2}^2\\
+36DaHa^2a + 800Da^2(1-\phi)^{5/2}Rd^2b(sin\gamma)^2\phi^3\alpha_1{\alpha_2}^2\\
-800Da^2(1-\phi)^{5/2}Rd^2b(sin\gamma)^2\phi^2\alpha_1{\alpha_2}^2\\
+80Da^2(1-\phi)^{5/2}Rd^2b(sin\gamma)^2\phi^5\alpha_1{\alpha_2}^2\\
-400Da^2(1-\phi)^{5/2}Rd^2b(sin\gamma)^2\phi^4\alpha_1{\alpha_2}^2\\
-45720Da^2PrRdb(sin\gamma)^2\phi^2{\alpha_2}^2\alpha_3 + 22860Da^2PrRdb(sin\gamma)^2\phi{\alpha_2}^2\alpha_3\\
+4572Da^2PrRdb(sin\gamma)^2\phi^5{\alpha_2}^2\alpha_3\\
-22860Da^2PrRdb(sin\gamma)^2\phi^4{\alpha_2}^2\alpha_3 + 45720Da^2PrRdb(sin\gamma)^2\phi^3{\alpha_2}^2\alpha_3\\
-24960Da^2Rda^3\phi^2{\alpha_1}^2 + 24960Da^2Rda^3\phi^3{\alpha_1}^2\\
-12480Da^2Rda^3\phi^4{\alpha_1}^2 + 2496Da^2Rda^3\phi^5{\alpha_1}^2 + 8320Da^2Rd^2a^3\phi{\alpha_1}^2\\
+181440Da^2Pra^3{\alpha_3}^2 + 48Rda\\
+16640Da^2Rd^2a^3\phi^3{\alpha_1}^2 - 16640Da^2Rd^2a^3\phi^2{\alpha_1}^2\\
-8320Da^2Rd^2a^3\phi^4{\alpha_1}^2 - 768Da(1-\phi)^{5/2}Rd^2a^2\alpha_1\\
+1664Da^2Rd^2a^3\phi^5{\alpha_1}^2 - 2496Da^2Rda^3{\alpha_1}^2 + 64DaHa^2Rd^2a\\
+32Da^2Ha^4Rd^2a - 1664Da^2Rd^2a^3{\alpha_1}^2
\end{array}\right)$$

In the same manner, the expressions for$\Theta[11]$,$\Theta[12]$, $\Theta[13]$, $\Theta[14]$, $\Theta[15]\ldots$ are found but they are too large to be included in this paper

From the definition of DTM, the solutions of Eqs. (2.13)and (2.14) are developed as

$$\begin{aligned} f(\eta) &= F[0] + \eta F[1] + \eta^2 F[2] + \eta^3 F[3] + +\eta^4 F[4] + \eta^5 F[5] \\ &+ \eta^6 F[6] + \eta^7 F[7] + \eta^8 F[8] + \eta^9 F[9] + +\eta^{10} F[10] + ... \end{aligned} \tag{3.7}$$

$$\begin{aligned} \theta(\eta) &= \Theta[0] + \eta\Theta[1] + \eta^2\Theta[2] + \eta^3\Theta[3] + +\eta^4\Theta[4] + \eta^5\Theta[5] \\ &+ \eta^6\Theta[6] + \eta^7\Theta[7] + \eta^8\Theta[8] + \eta^9\Theta[9] + +\eta^{10}\Theta[10] + ... \end{aligned} \tag{3.8}$$

International Journal of Mathematical Analysis and Optimization: Theory and Applications
Vol. 2020, No. 1, pp. 780 - 799

Now, consider similar fully coupled third and second orders ordinary differential equations presented in Eqs. (2.13) and (2.14), but at this time, we take *a=1* and *b=1*

$$g'''(\eta)+(1-\phi)^{2.5}\left\{\begin{array}{l}\alpha_1\left(3g(\eta)\,g''(\eta)-2\,(f'(\eta))^2\right)+\alpha_2\vartheta(\eta)\cos\gamma\\-\left(M^2+Da^{-1}\right)g(\eta)\end{array}\right\}=0 \tag{3.9}$$

$$\vartheta''(\eta)+3\alpha_3Prg(\eta)\,\vartheta'(\eta)=0 \tag{3.10}$$

With initial conditions as

$$g=0,\quad g'=0,\quad g''=1,\quad \vartheta=1,\quad \vartheta'=1\quad when\;\eta=0 \tag{3.11}$$

Following the similar solution procedures of Eqs. (2.13) and (2.14), the solutions of Eqs. (3.9) and (3.10) are

$$\begin{array}{c}g(\eta)=G[0]+\eta G[1]+\eta^2G[2]+\eta^3G[3]++\eta^4G[4]+\eta GF[5]\\+\eta^6G[6]+\eta^7G[7]+\eta^8G[8]+\eta^9G[9]++\eta^{10}G[10]+...\end{array} \tag{3.12}$$

and

$$\begin{array}{c}\vartheta(\eta)=\Phi[0]+\eta\Phi[1]+\eta^2\Phi[2]+\eta^3\Phi[3]++\eta^4\Phi[4]+\eta^5\Phi[5]\\+\eta^6\Phi[6]+\eta^7\Phi[7]+\eta^8\Phi[8]+\eta^9\Phi[9]++\eta^{10}\Phi[10]+...\end{array} \tag{3.13}$$

where

$$G[0]=0,\quad G[1]=0,\quad ,G[2]=\frac{1}{2},\quad \theta[0]=1,\quad \theta[1]=1$$

$$G[3]=-\frac{1}{6}(1-\phi)^{5/2}\alpha_2\sin\gamma$$

$$G[4]=-\frac{1}{24}(1-\phi)^{5/2}\alpha_2\sin\gamma$$

$$G[5]=\frac{\left(2(1-\phi)^{5/2}\alpha_1Da+Ha^2Da+1\right)}{60Da}$$

$$G[6]=-\frac{\left(DaHa^2+1\right)(1-\phi)^{5/2}\alpha_2\sin\gamma}{720Da}$$

$$G[7]=-\frac{(1-\phi)^{5/2}\alpha_2b\sin\gamma\left(\begin{array}{c}-40Da(1-\phi)^{5/2}Rd\alpha_1-30(1-\phi)^{5/2}\alpha_1Da\\+4DaHa^2Rd-18DaPr\alpha_3+3DaHa^2+4Rd+3\end{array}\right)}{(15120+20160Rd)\,Da}$$

International Journal of Mathematical Analysis and Optimization: Theory and Applications
Vol. 2020, No. 1, pp. 780 - 799

$$G\left[8\right]=\frac{1}{\left(120960+161280Rd\right)Da^2}\left(\begin{array}{l}6a+8Da^2Ha^4Rda+16DaHa^2Rda-144\left(1-\phi\right)^{5/2}\alpha_1Da+312Da^2\phi^5{\alpha_1}^2\\-1560Da^2\phi^4{\alpha_1}^2+3120Da^2\phi^3{\alpha_1}^2-3120Da^2\phi^2{\alpha_1}^2+1560Da^2\phi{\alpha_1}^2\\-416Da^2Rd{\alpha_1}^2-192Da^2Ha^2\left(1-\phi\right)^{5/2}Rd\alpha_1\\-15Da^2\left(1-\phi\right)^{5/2}\left(sin\gamma\right)^2\alpha_1{\alpha_2}^2-9Da^2Prb\left(sin\gamma\right)^2{\alpha_2}^2\alpha_3\\+100Da^2\left(1-\phi\right)^{5/2}Rd\left(sin\gamma\right)^2\phi\alpha_1{\alpha_2}^2\\-200Da^2\left(1-\phi\right)^{5/2}Rd\left(sin\gamma\right)^2\phi^2\alpha_1{\alpha_2}^2\\-100Da^2\left(1-\phi\right)^{5/2}Rd\left(sin\gamma\right)^2\phi^4\alpha_1{\alpha_2}^2\\+200Da^2\left(1-\phi\right)^{5/2}Rd\left(sin\gamma\right)^2\phi^3\alpha_1{\alpha_2}^2\\+20Da^2\left(1-\phi\right)^{5/2}Rd\left(sin\gamma\right)^2\phi^5\alpha_1{\alpha_2}^2-192Da\left(1-\phi\right)^{5/2}Rd\alpha_1\\-144Da^2Ha^2\left(1-\phi\right)^{5/2}\alpha_1-4160Da^2Rd\phi^2{\alpha_1}^2\\+2080Da^2Rd\phi{\alpha_1}^2+4160Da^2Rd\phi^3{\alpha_1}^2+416Da^2Rd\phi^5{\alpha_1}^2\\-2080Da^2Rd\phi^4{\alpha_1}^2+8Rd+12DaHa^2-312Da^2{\alpha_1}^2\\+6Da^2Ha^4-20Da^2\left(1-\phi\right)^{5/2}Rd\left(sin\gamma\right)^2\alpha_1{\alpha_2}^2\\+75Da^2\left(1-\phi\right)^{5/2}\left(sin\gamma\right)^2\phi\alpha_1{\alpha_2}^2+150Da^2\left(1-\phi\right)^{5/2}\left(sin\gamma\right)^2\phi^3\alpha_1{\alpha_2}^2\\-150Da^2\left(1-\phi\right)^{5/2}\left(sin\gamma\right)^2\phi^2\alpha_1{\alpha_2}^2+15Da^2\left(1-\phi\right)^{5/2}\left(sin\gamma\right)^2\phi^5\alpha_1{\alpha_2}^2\\-75Da^2\left(1-\phi\right)^{5/2}\left(sin\gamma\right)^2\phi^4\alpha_1{\alpha_2}^2+9Da^2Pr\left(sin\gamma\right)^2\phi^5{\alpha_2}^2\alpha_3\\-45Da^2Pr\left(sin\gamma\right)^2\phi^4{\alpha_2}^2\alpha_3+90Da^2Pr\left(sin\gamma\right)^2\phi^3{\alpha_2}^2\alpha_3\\-90Da^2Pr\left(sin\gamma\right)^2\phi^2{\alpha_2}^2\alpha_3+45Da^2Pr\left(sin\gamma\right)^2\phi{\alpha_2}^2\alpha_3\end{array}\right)$$

$$G\left[9\right]=-\frac{\left(1-\phi\right)^{5/2}\alpha_2sin\gamma}{\left(1088640+1451520Rd\right)Da^2}\left(\begin{array}{l}3-252\left(1-\phi\right)^{5/2}\alpha_1Da+216Da^2\phi^5{\alpha_1}^2-1080Da^2\phi^4{\alpha_1}^2\\+2160Da^2\phi^3{\alpha_1}^2-2160Da^2\phi^2{\alpha_1}^2+1080Da^2\phi{\alpha_1}^2\\-288Da^2Rd{\alpha_1}^2-15Da^2\phi^5\alpha_1\alpha_2sin\gamma+75Da^2\phi^4\alpha_1\alpha_2sin\gamma\\-150Da^2\phi^3\alpha_1\alpha_2sin\gamma+150Da^2\phi^2\alpha_1\alpha_2sin\gamma+20Da^2Rd\alpha_1\alpha_2sin\gamma\\-75Da^2\phi\alpha_1\alpha_2sin\gamma-336Da^2Ha^2\left(1-\phi\right)^{5/2}Rda\alpha_1\\+8DaHa^2Rd+200Da^2Rd\phi^2\alpha_1\alpha_2sin\gamma+100Da^2Rd\phi^4\alpha_1\alpha_2sin\gamma\\-1440Da^2Rd\phi^4{\alpha_1}^2-200Da^2Rd\phi^3\alpha_1\alpha_2sin\gamma\\+9Da^2\left(1-\phi\right)^{5/2}Pr\alpha_2\alpha_3sin\gamma-20Da^2Rd\phi^5\alpha_1\alpha_2sin\gamma\\-100Da^2Rd\phi\alpha_1\alpha_2sin\gamma-336Da(1-\phi)^{5/2}Rd\alpha_1+\\288Da^2Rd\phi^5\alpha_1^2+15Da^2\alpha_1\alpha_2sin\gamma-252Da^2Ha^2(1-\phi)^{5/2}\alpha_1\\-2880Da^2Rd\phi^2\alpha_1^2+1440Da^2Rd\phi\alpha_1^2+2880Da^2Rd\phi^2\alpha_1^2\\+6Ha^2Da+3Da^2Ha^4+4Da^2Ha^4Rd-216Da^2\alpha_1^2+4Rd\end{array}\right)$$

International Journal of Mathematical Analysis and Optimization: Theory and Applications
Vol. 2020, No. 1, pp. 780 - 799

$$G[10]=-\frac{(1-\phi)^{5/2}\alpha_2 sin\gamma}{(3628800(3+4Rd)^2)Da^2}\left(\begin{array}{l}-77760Da^2Rd\phi{\alpha_1}^2+9+5832Da^2{\alpha_1}^2+16Da^2Ha^4Rd^2+24Da^2Ha^4Rd\\+32DaHa^2Rd^2+48DaHa^2Rd+378Da\alpha_1\alpha_2 sin\gamma\\-378Da^2Ha^2\phi^5\alpha_1\alpha_2 sin\gamma+1890Da^2Ha^2\phi^4\alpha_1\alpha_2 sin\gamma\\-672DaRd^2\phi^5\alpha_1\alpha_2 sin\gamma-3780Da^2Ha^2\phi^3\alpha_1\alpha_2 sin\gamma\\+3360DaRd^2\phi^4\alpha_1\alpha_2 sin\gamma-1008DaRd\phi^5\alpha_1\alpha_2 sin\gamma\\+672Da^2Ha^2Rd^2\alpha_1\alpha_2 sin\gamma-6720DaRd^2\phi^3\alpha_1\alpha_2 sin\gamma\\+5040DaRd\phi^4\alpha_1\alpha_2 sin\gamma-10368Da^2Rd^2\phi^5{\alpha_1}^2\\+51840Da^2Rd^2\phi^4{\alpha_1}^2-15552Da^2Rd\phi^5{\alpha_1}^2\\-103680Da^2Rd^2\phi^3{\alpha_1}^2+77760Da^2Rd\phi^4{\alpha_1}^2\\+103680Da^2Rd^2a^2b\phi^2{\alpha_1}^2-155520Da^2Rd\phi^3{\alpha_1}^2\\-51840Da^2Rd^2\phi{\alpha_1}^2+155520Da^2Rd\phi^2{\alpha_1}^2\\+5328Da^2(1-\phi)^{5/2}PrRd\alpha_1\alpha_3+3780Da\phi^2\alpha_1\alpha_2 sin\gamma\\+672DaRd^2\alpha_1\alpha_2 sin\gamma+378Da^2Ha^2\alpha_1\alpha_2 sin\gamma\\+3360Da^2Ha^2Rd^2\phi^4\alpha_1\alpha_2 sin\gamma-3780Da\phi^3\alpha_1\alpha_2 sin\gamma\\+1890Da\phi^4\alpha_1\alpha_2 sin\gamma+3240Da^2Pr{\alpha_3}^2-378Da\phi^5\alpha_1\alpha_2 sin\gamma\\+10080Da^2Ha^2Rd\phi^2\alpha_1\alpha_2 sin\gamma-3360Da^2Ha^2Rd^2\phi\alpha_1\alpha_2 sin\gamma\\-10080Da^2Ha^2Rd\phi^3\alpha_1\alpha_2 sin\gamma+6720Da^2Ha^2Rd^2\phi^2\alpha_1\alpha_2 sin\gamma\\+5040Da^2Ha^2Rd sin\gamma\phi^4\alpha_1\alpha_2-6720Da^2Ha^2Rd^2 sin\gamma\phi^3\alpha_1\alpha_2\\-1008Da^2Ha^2Rd\phi^5\alpha_1\alpha_2 sin\gamma-3408Da(1-\phi)^{5/2}Rd\alpha_1\\+3780Da^2Ha^2\phi^2\alpha_1\alpha_2 sin\gamma-2272Da(1-\phi)^{5/2}Rd^2\alpha_1\\-1278Da^2Ha^2(1-\phi)^{5/2}\alpha_1-5040DaRd\phi\alpha_1\alpha_2 sin\gamma\\-144DaPrRd\alpha_3+10080DaRd\phi^2\alpha_1\alpha_2 sin\gamma-3360DaRd^2\phi\alpha_1\alpha_2 sin\gamma\\-10080DaRd\phi^3\alpha_1\alpha_2 sin\gamma+6720DaRd^2\phi^2\alpha_1\alpha_2 sin\gamma\\-1890Da^2Ha^2\phi\alpha_1\alpha_2 sin\gamma+1008Da^2Ha^2Rd\alpha_1\alpha_2 sin\gamma\\-672Da^2Ha^2Rd^2\phi^5\alpha_1\alpha_2 sin\gamma-108Da^2Ha^2Pr\alpha_3+9Da^2Ha^4\\+18DaHa^2-1278Da(1-\phi)^{5/2}\alpha_1-108DaPr\alpha_3+1008DaRd\alpha_1\alpha_2 sin\gamma\\-1890Da\phi\alpha_1\alpha_2 sin\gamma+58320Da^2a^2\phi^2{\alpha_1}^2-29160Da^2\phi{\alpha_1}^2\\+29160Da^2\phi^4{\alpha_1}^2-58320Da^2\phi^3{\alpha_1}^2-5832Da^2\phi^5{\alpha_1}^2\\+10368Da^2Rd^2{\alpha_1}^2+15552Da^2Rd{\alpha_1}^2+16Rd^2+24Rd\\-5040Da^2Ha^2Rd\phi\alpha_1\alpha_2 sin\gamma-144Da^2Ha^2PrRd\alpha_3\\+3996Da^2(1-\phi)^{5/2}Pr\alpha_1\alpha_3-3408Da^2Ha^2(1-\phi)^{5/2}Rd\alpha_1\\-2272Da^2Ha^2(1-\phi)^{5/2}Rd^2\alpha_1\end{array}\right)$$

Similarly

$$\Phi[2]=0$$

$$\Phi[3]=0$$

$$\Phi[4]=-\frac{3}{4}\left(\frac{\alpha_3 Pr}{3+4Rd}\right)$$

$$\Phi[5]=\frac{3\alpha_3 Pr(1-\phi)^{5/2}\alpha_2 sin\gamma}{120+160Rd}$$

$$\Phi[6]=\frac{\alpha_3 Pr(1-\phi)^{5/2}\alpha_2 sin\gamma}{240+320Rd}$$

$$\Phi[7]=-\frac{\alpha_3 Pr\left(\begin{array}{l}3+8Da(1-\phi)^{5/2}Rd\alpha_1+6(1-\phi)^{5/2}\alpha_1 Da\\+4DaHa^2Rd-180DaPr\alpha_3+3DaHa^2+4Rd\end{array}\right)}{280(3+4Rd)^2 Da}$$

INTERNATIONAL JOURNAL OF MATHEMATICAL ANALYSIS AND OPTIMIZATION: THEORY AND APPLICATIONS
VOL. 2020, NO. 1, PP. 780 - 799

$$\Phi[8]=\frac{\alpha_3 Pr\left(1-\phi\right)^{5/2}\alpha_2\left(4DaHa^2Rd-630DaPr\alpha_3+3DaHa^2+4Rd+3\right)sin\gamma}{4480\left(3+4Rd\right)^2 Da}$$

$$\Phi[9]=\frac{\alpha_3 Pr\alpha_2 sin\gamma}{40320\left(3+4Rd\right)^2 Da}\left(\begin{array}{l}
4DaHa^2\left(1-\phi\right)^{5/2}Rd-1026\alpha_3Pr\left(1-\phi\right)^{5/2}Da-315DaPr\phi^5\alpha_2\alpha_3sin\gamma\\
+40DaRd\phi^5\alpha_1+3DaHa^2\left(1-\phi\right)^{5/2}+1575DaPr\phi^4\alpha_2\alpha_3sin\gamma\\
-200DaRd\phi^4\alpha_1+30Da\phi^5\alpha_1+150Da\phi\alpha_1-30Da\alpha_1\\
-3150DaPr\phi^3\alpha_2\alpha_3sin\gamma+400DaRd\phi^3\alpha_1-150Da\phi^4\alpha_1\\
+3150DaPr\phi^2\alpha_2\alpha_3sin\gamma-400DaRd\phi^2\alpha_1+300Da\phi^3\alpha_1\\
+4\left(1-\phi\right)^{5/2}Rd-1575DaPr\phi\alpha_2\alpha_3sin\gamma+200DaRd\phi\alpha_1\\
-300Da\phi^2\alpha_1+3\left(1-\phi\right)^{5/2}+315\alpha_3Pr\alpha_2Dasin\gamma-40DaRd\alpha_1
\end{array}\right)$$

$$\Phi[10]=-\frac{\alpha_3 Pr}{403200(3+4Rd)^3Da^2}\left(\begin{array}{l}
-1152Da^2Ha^2\left(1-\phi\right)^{5/2}Rd\alpha_1-450Da^2\left(1-\phi\right)^{5/2}\left(sin\gamma\right)^2\phi^2\alpha_1{\alpha_2}^2\\
+18-9072\alpha_3PrDa+48Da^2Ha^4Rd+96DaHa^2Rd\\
-432\left(1-\phi\right)^{5/2}\alpha_1Da+936Da^2\phi^5{\alpha_1}^2-4680Da^2\phi^4{\alpha_1}^2\\
+9360Da^2\phi^3{\alpha_1}^2-9360Da^2\phi^2{\alpha_1}^2+4680Da^2\phi{\alpha_1}^2\\
-45Da^2\left(1-\phi\right)^{5/2}\left(sin\gamma\right)^2\alpha_1{\alpha_2}^2-12096Da^2Ha^2PrRda^2\alpha_3\\
-18144Da^2\left(1-\phi\right)^{5/2}Pr\alpha_1\alpha_3-768Da^2Ha^2\left(1-\phi\right)^{5/2}Rd^2\alpha_1\\
-12096DaPrRd\alpha_3-9072Da^2Ha^2Pr\alpha_3\\
+450Da^2\left(1-\phi\right)^{5/2}\left(sin\gamma\right)^2\phi^3\alpha_1{\alpha_2}^2-225Da^2\left(1-\phi\right)^{5/2}\left(sin\gamma\right)^2\phi^4\alpha_1{\alpha_2}^2\\
+45Da^2\left(1-\phi\right)^{5/2}\left(sin\gamma\right)^2\phi^5\alpha_1{\alpha_2}^2+3429Da^2Pr\left(sin\gamma\right)^2\phi^5{\alpha_2}^2\alpha_3\\
+34290Da^2Pr\left(sin\gamma\right)^2\phi^3{\alpha_2}^2\alpha_3-34290Da^2Pr\left(sin\gamma\right)^2\phi^2{\alpha_2}^2\alpha_3\\
-80Da^2\left(1-\phi\right)^{5/2}Rd^2\left(sin\gamma\right)^2\alpha_1{\alpha_2}^2-4572Da^2PrRd\left(sin\gamma\right)^2{\alpha_2}^2\alpha_3\\
-17145Da^2Pr\left(sin\gamma\right)^2\phi^4{\alpha_2}^2\alpha_3-120Da^2\left(1-\phi\right)^{5/2}Rd\left(sin\gamma\right)^2\alpha_1{\alpha_2}^2\\
-24192Da^2\left(1-\phi\right)^{5/2}PrRd\alpha_1\alpha_3+225Da^2\left(1-\phi\right)^{5/2}\left(sin\gamma\right)^2\phi\alpha_1{\alpha_2}^2\\
+600Da^2\left(1-\phi\right)^{5/2}Rd\left(sin\gamma\right)^2\phi\alpha_1{\alpha_2}^2\\
-1200Da^2\left(1-\phi\right)^{5/2}Rd\left(sin\gamma\right)^2\phi^2\alpha_1{\alpha_2}^2\\
+1200Da^2\left(1-\phi\right)^{5/2}Rd\left(sin\gamma\right)^2\phi^3\alpha_1{\alpha_2}^2\\
-600Da^2\left(1-\phi\right)^{5/2}Rd\left(sin\gamma\right)^2\phi^4\alpha_1{\alpha_2}^2\\
+120Da^2\left(1-\phi\right)^{5/2}Rd\left(sin\gamma\right)^2\phi^5\alpha_1{\alpha_2}^2+32Rd^2+18Da^2Ha^4\\
-1152Da\left(1-\phi\right)^{5/2}Rd\alpha_1-432Da^2Ha^2\left(1-\phi\right)^{5/2}\alpha_1+12480Da^2Rd\phi{\alpha_1}^2\\
-936Da^2{\alpha_1}^2-3429Da^2Pr\left(sin\gamma\right)^2{\alpha_2}^2\alpha_3+17145Da^2Pr\left(sin\gamma\right)^2\phi{\alpha_2}^2\alpha_3\\
+400Da^2\left(1-\phi\right)^{5/2}Rd^2\left(sin\gamma\right)^2\phi\alpha_1{\alpha_2}^2+36DaHa^2\\
+800Da^2\left(1-\phi\right)^{5/2}Rd^2\left(sin\gamma\right)^2\phi^3\alpha_1{\alpha_2}^2\\
-800Da^2\left(1-\phi\right)^{5/2}Rd^2\left(sin\gamma\right)^2\phi^2\alpha_1{\alpha_2}^2\\
+80Da^2\left(1-\phi\right)^{5/2}Rd^2\left(sin\gamma\right)^2\phi^5\alpha_1{\alpha_2}^2\\
-400Da^2\left(1-\phi\right)^{5/2}Rd^2\left(sin\gamma\right)^2\phi^4\alpha_1{\alpha_2}^2-45720Da^2PrRd\left(sin\gamma\right)^2\phi^2{\alpha_2}^2\alpha_3\\
+22860Da^2PrRd\left(sin\gamma\right)^2\phi{\alpha_2}^2\alpha_3+4572Da^2PrRd\left(sin\gamma\right)^2\phi^5{\alpha_2}^2\alpha_3\\
-22860Da^2PrRd\left(sin\gamma\right)^2\phi^4{\alpha_2}^2\alpha_3+45720Da^2PrRd\left(sin\gamma\right)^2\phi^3{\alpha_2}^2\alpha_3\\
-24960Da^2Rd\phi^2{\alpha_1}^2+24960Da^2Rd\phi^3{\alpha_1}^2-12480Da^2Rd\phi^4{\alpha_1}^2\\
+2496Da^2Rd\phi^5{\alpha_1}^2+8320Da^2Rd^2\phi{\alpha_1}^2+181440Da^2Pr{\alpha_3}^2+48Rd\\
+16640Da^2Rd^2\phi^3{\alpha_1}^2-16640Da^2Rd^2\phi^2{\alpha_1}^2-8320Da^2Rd^2\phi^4{\alpha_1}^2\\
-768Da\left(1-\phi\right)^{5/2}Rd^2\alpha_1+1664Da^2Rd^2\phi^5{\alpha_1}^2-2496Da^2Rd{\alpha_1}^2\\
+64DaHa^2Rd^2+32Da^2Ha^4Rd^2a-1664Da^2Rd^2{\alpha_1}^2
\end{array}\right)$$

The functions in Eq. (3.9) and (3.10) and that in Eq. (3.12) and (3.13) have relations as follows:

$$f(\eta)=a^kg(a^q\eta)\rightarrow f'(\eta)=a^{k+q}g'(a^q\eta)\rightarrow f'(\infty)=a^{k+q}g'(\infty) \tag{3.14}$$

International Journal of Mathematical Analysis and Optimization: Theory and Applications
Vol. 2020, No. 1, pp. 780 - 799

and

$$\theta(\eta) = b'\vartheta(b^s\eta) \rightarrow \theta(\infty) = b'\vartheta(\infty) \tag{3.15}$$

From Eq. (2.12), $f'(\infty) = 0$ and $\theta(\infty) = b'\vartheta(\infty)$
Since $a \neq 0$ and $b \neq 0 \rightarrow g'(\infty) = 0$ and $\vartheta(\infty) = 0$.

4 Applying Multi-step DTM

The domain $[0, \infty)$ is replaced by $[0, \eta_\infty)$. The solution domain is divided to N equal parts ($H = \eta_\infty/N$). Therefore, one can write

$$g_i'''(\eta_i) + (1-\phi)^{2.5}\left\{\begin{array}{l} \left[(1-\phi)+\phi\left(\frac{\rho_s}{\rho_t}\right)\right]\left(3g_i(\eta_i)g_i'''(\eta_i) - 2\left(g_i^1(\eta_i)\right)^2\right) \\ +\left[(1-\phi)+\phi\left[\frac{(\rho\beta)_s}{(\rho\beta)_t}\right]\right]\vartheta_i(\eta_i)\cos\gamma \\ -(M^2+Da^{-1})g_i(\eta_i) \end{array}\right\} = 0 \tag{4.1}$$

$$(i-1)H \leq \eta_i < iH, \quad for \;\; i \leq i \leq N.$$

$$\vartheta_i'(\eta_i) + 3\left[\frac{1}{\left[(1-\phi)+\phi\left[\frac{(\rho C_p)_s}{(\rho C_p)_t}\right]\right]}\left[\frac{k_s+(m-1)k_t-(m-1)\phi(k_t-k_s)}{k_s+(m-1)k_t+\phi(k_t-k_s)}\right]\right] Pr g_i(\eta_i)\vartheta_i(\eta_i) = 0 \tag{4.2}$$

With the application of multi-step DTM on Eq. (4.1) and Eq. (4.2)

$$G_i(p+3) = \frac{(1-\phi)^{2.5}H^3}{(p+1)(p+2)(p+3)}\left\{\begin{array}{l} \alpha_1\left[\begin{array}{l} 2\sum_{i=0}^{p}\frac{(l+1)}{H}G_i(l+1)\frac{(p-l+1)}{H}G_i(p-l+1) \\ -3\sum_{i=0}^{p}G_i(l)\frac{(p-l+1)(p-l+2)}{H^2}G_i(p-l+2) \end{array}\right] \\ -\alpha_2\vartheta_i(p)cos\gamma - (M^2+Da^{-1})G_i(p) \end{array}\right\} \tag{4.3}$$

$$\vartheta_i(p+2) = \frac{-3H^2 Pr}{(p+1)(p+2)}\left\{\alpha_3\sum_{i=0}^{p}\frac{(l+1)}{H}\vartheta_i(l+1)G_i(p-l)\right\} \tag{4.4}$$

for $i \leq i \leq N$.
The initial conditions are considered for the first sub dormain ($i = 1$). The differential transform for the initial conditions are

$$\begin{array}{l} G_1(0) = g_1(0) = 0, \quad G_1(1) = Hg_1'(0) = 0, \quad G_1(2) = \frac{H^2}{2}g_1'' = \frac{H^2}{2}, \\ \psi_1(0) = \vartheta_1(0) = 1, \quad \psi_1(1) = H\vartheta(0) = H \end{array} \tag{4.5}$$

The boundary conditions of each subdormain are continuity of the

$$g_i(\eta_i), \quad g_i'(\eta_i), \quad g_i''(\eta_i), \quad \vartheta(\eta_i), \quad \vartheta(\eta_i) \tag{4.6}$$

The above boundary conditions can be obtained as

$$\begin{array}{l} g_i(\eta_{i+1}) = \sum_{k=0}^{m}G_i(k) \\ g_{i+1}(\eta_{i+1}) = G_{i+1}(0) \rightarrow G_{i+1}(0) = \sum_{k=0}^{m}G_i(k) \end{array} \tag{4.7}$$

$$\begin{aligned} g_i'(\eta_{i+1}) &= \sum_{k=1}^{m} \frac{k}{H} G_i(k) \\ g_i'(\eta_{i+1}) &= \frac{G_{i+1}(1)}{H} \rightarrow G_{i+1}(1) = \sum_{k=1}^{m} k G_i(k) \end{aligned} \tag{4.8}$$

$$\begin{aligned} g_i''(\eta_{i+1}) &= \sum_{k=2}^{m} \frac{k(k-1)}{H} G_i(k) \\ g_i''(\eta_{i+1}) &= \frac{2G_{i+1}(2)}{H} \rightarrow G_{i+1}(2) = \frac{1}{2} \sum_{k=1}^{m} k(k-1) G_i(k) \end{aligned} \tag{4.9}$$

$$\begin{aligned} \vartheta_i(\eta_{i+1}) &= \sum_{k=0}^{m} \psi_i(k) \\ \vartheta_{i+1}(\eta_{i+1}) &= \psi_{i+1}(0) \rightarrow \psi_{i+1}(0) = \sum_{k=0}^{m} \psi_i(k) \end{aligned} \tag{4.10}$$

$$\begin{aligned} \vartheta_i(\eta_{i+1}) &= \sum_{k=1}^{m} \frac{k}{H} \psi_i(k) \\ \vartheta_i(\eta_{i+1}) &= \frac{\psi_{i+1}(1)}{H} \rightarrow \psi_{i+1}(1) = \sum_{k=1}^{m} k \psi_i(k) \end{aligned} \tag{4.11}$$

The values of the $g'(\eta_\infty)$ and $\vartheta(\eta_\infty)$ are calculated as

$$\begin{aligned} g_i'(\infty) &\simeq g_i'(\eta_\infty) = g_i'(\eta_{N+1}) = \sum_{k=1}^{m} \frac{k}{H} G_N(k) \\ \vartheta_i(\infty) &\simeq \vartheta_i(\eta_\infty) = \vartheta_i(\eta_{N+1}) = \sum_{k=0}^{m} \psi_N(k) \end{aligned} \tag{4.12}$$

Now, Eq. (2.13) and (2.14) are solved with a similar process like Eqs. (4.1) and (4.2) using the multistep DTM. The only difference is that the condition $f''(0) = a$ is replaced by the condition $g''(0) = 1$.

5 Results and Discussion

Comparison of present results with the results in literature are shown in Table 1. the past works are of viscous fluid where the volume fraction of the nanoparticle is zero ($\phi = 0$). The excellent agreements between the results show the high accuracy of the developed solution by the method in the present study. the table presents the effects of Prandti number on the viscous fluid flow process.

Table 1: Comparison of results for the skin friction parameter when $\phi = 0$

	$f''(0)$		
Pr	Sparrow & Gregg[5]	Kuiken[8]	Present study
0.003 0224	1.0223	1.0151	1.
0.008	0.9955	0.9801	0.9955
0.020	0.9590	0.9284	0.9591
1.30	0.9384	0.8966	0.9384

5.1 Impact of plate inclination on nanofluid velocity and temperature distributions

Fig. 3 and 4 shows the impacts of flat plate inclination on the nanofuid flow velocity and temperature profiles. It is shown in the figures that as the plate inclination (angle of inclination to the horizontal of the stretching sheet), γ increases, there is recorded increase in the nanofluid flow velocity and the flow is increasingly accelerated. This is because, increasing the inclined surface angle strengthens the buoyancy term and the buoyancy force become more pronounced as well as the wall shear force become increased. This leads to increase in the free flow of the fluid which consequently, increase the fluid velocity and decrease fluid temperature within the boundary layer as the momentum boundary layer becomes thicker (increase in the momentum boundary layer thickness). However, the thermal boundary layer turns out to be slightly thinner (the thermal boundary layer thickness decreases) due to the increased inclination of the flat surface.
Also, from the governing equations, the angle of inclination, γ appears only in the buoyancy term (as $\sin\gamma$) of the momentum equation. Therefore, the gravitational effect as well as the flow velocity of the fluid attains its maximum values when the plate assumes vertical position i.e when the angle of inclination of the plate, $\gamma = \pi/2$ and the effect of gravity on the flow and the flow velocity reaches minimum values when $\gamma = 0$ i.e when the plate assumes horizontal position. The horizontal and vertical position of the plate are the limiting cases of the inclined stretching sheet problem. The results clearly reveal that the inclination of the stretching sheet can be effectively used to obtain a desired temperature.

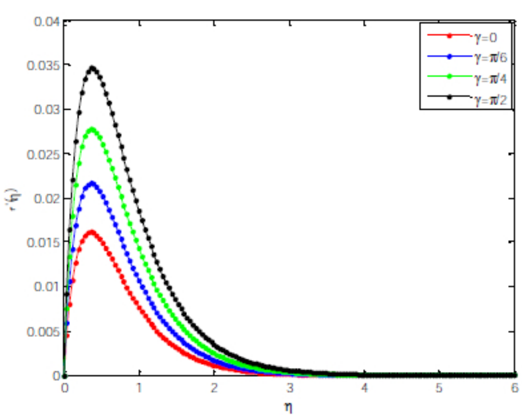

Figure 3: Effects of inclination angle on velocity profile

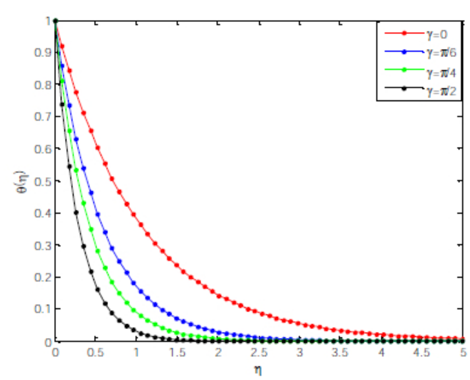

Figure 4: Effects of inclination angle on temperature profile

5.2 Impact of magnetic field on nanofluid velocity and temperature distributions

Although the flow of the fluid is enhanced with the flow medium porosity or permeability, the magnetic field strength is very effective in retarding and controlling the flow of the fluid as the velocity of the fluid decreases as the strength of the magnetic field increases. However, increase magnetic field results in increase temperature of the fluid within the boundary layer. This is due to the interaction of magnetic field with nanofluid particles which generates heat in the fluid region and creates a hot fluid layer within the boundary layer. It should also be added that the magnetic force reduces the temperature difference between the plate and ambient fluid. The effects of nanoparticles on fluid velocity and heat transfer show that as the concentration of the nanoparticle in the base fluid increases, the velocity of the fluid decreases and the temperature increases due to the increase

IJMAO
International Journal of Mathematical Analysis and Optimization: Theory and Applications
Vol. 2020, No. 1, pp. 780 - 799

in shear stress, skin friction and the thickness of thermal boundary layer.

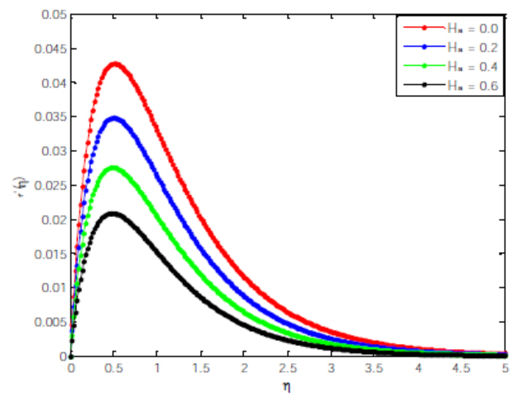

Figure 5: Effects of magnetic field on the velocity profile

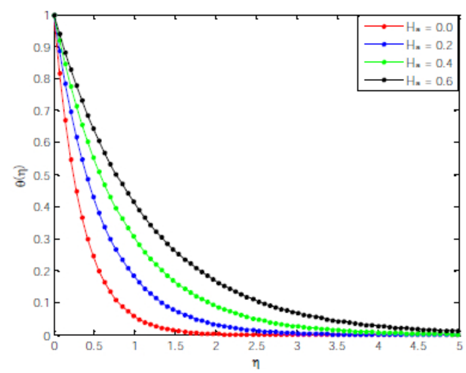

Figure 6: Effects of magnetic field on temperature profile

5.3 Impact of thermal radiation parameter on nanofluid velocity and temperature distributions

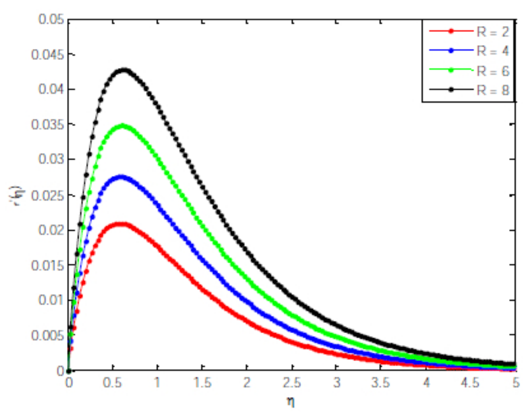

Figure 7: Effects of radiation parameter on the velocity profile of the nanofluid

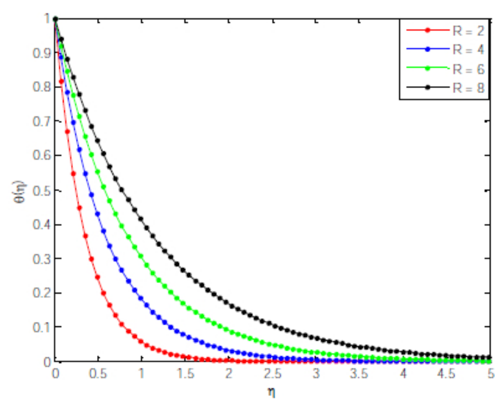

Figure 8: Effects of radiation parameter on temperature profile of the nanofluid

Figs. 7 and 8 illustrates the effects of thermal radiation on the nanofluid flow velocity and temperature. The figure reveals that as the thermal radiation increases, the velocity and temperature of the fluid increase which infer that both viscous and thermal boundary layers increase with the increase in thermal radiation parameter. This is because as the radiation is increased, the heated plate releases more heat energy released to the fluid in both momentum and thermal boundary layers. This consequently increases the buoyancy force and the momentum boundary layer thereby the fluid motion is augmented and the temperature is enhanced.

6 Conclusion

In this work, the coupled effects of stretching plate inclination, magnetic field and thermal radiation on natural convection heat transfer of nanofluid over a surface have been investigated theoretically using multi-step differential transformation method. From the parametric studies, the following observations were established.

(i) The velocity of the fluid increase as the plate inclination, γ increases. Also, the flow velocity of the fluid attains maximum value when the plate inclination, $\gamma = \pi/2$ and the fluid velocity reaches minimum value when the plate inclination, $\gamma = 0$.

(ii) The fluid temperature decreases as the plate inclination, γ increases. Also, the flow velocity of the fluid attains minimum value when the plate inclination, $\gamma = \pi/2$ and the fluid velocity reaches maximum value when the plate inclination, $\gamma = 0$.

(iii) The velocity of the fluid decrease while the temperature increase as the magnetic field strength increase.

(iv) The viscous and thermal boundary layers increase with the increase of radiation parameter.

The study will help in such understanding nanofluid flow over a flat surface, design of flow equipment and controlling of the flow over flat surfaces.

Nomenclature

C_p specific heat capacity
k thermal conductivity
m shape factor
Pr Prandti factor
u velocity component in x-direction
v velocity component in z-direction
y axis perpendicular to plates
x axis along the horizontal direction
y axis along the vertical direction

Symbols

β volumetric extension coefficients
ρ density of the fluid
μ dynamic viscosity
η similarity variable
λ sphericity
ϕ volume fraction or concentration of the nanofluid
θ Dimensionless temperature

Subscript

f fluid
s solid
nf nanofluid

International Journal of Mathematical Analysis and Optimization: Theory and Applications
Vol. 2020, No. 1, pp. 780 - 799

References

[1] Schmidt, E. & Beckmann, W. Das temperatur-und geschwinigkeitsfeld vor einnar warme abgebenden senkrecher platte bei natürelicher convention. **1(10)**, 341–349 (1930); cont. **1(11)**, 391–406 (1930).

[2] Ostrach, S. An analysis of laminar free-convection flow and heat transfer about a flat plate parallel to the direction of the generating body force. *NACA Report* **1111**, (1953).

[3] Sparrow, E. M. & Gregg, J. L. Laminar free convection from a vertical plate with uniform surface heat flux. *Trans. A. S. M. E.* **78**, 435–440 (1956).

[4] Lefevre, E. J. Laminar free convection from a vertical plane surface. *9th Intern. Congresson Applied Mechanics, Brussels* **168**, (1956).

[5] Sparrow, E. M. & Gregg, J. L. Similar solutions for free convection from a nonisothermal vertical plate. *Trans. A.S.M.E.* **78**, 379–386 (1958).

[6] Stewartson, K. & Jones, L. T. The heated vertical plate at high Prandtl number. *J. Aeronautical Sciences* **24**, 379–380 (1957).

[7] Kuiken, H. K. An asymptotic solution for large Prandtl number free convection. *J. Engng. Math.* **2**, 355-371 (1968).

[8] Kuiken, H. K. Free convection at low Prandtl numbers. *J. Fluid Mech.* **37**, 785–798 (1969).

[9] Eshghy, S. Free-convection layers at large Prandtl number. *J. Applied Math. and Physics(ZAMP)* **22**, 275–292 (1971).

[10] Roy, S. High Prandtl number free convection for uniform surface heat flux. *Trans. A.S.M.E.J. Heat Transfer* **95**, 124–126 (1973).

[11] Kuiken, H. K. & Rotem, Z. Asymptotic solution for the plume at very large and small Prandtl numbers. *J. Fluid Mech.* **45**, 585–600 (1971).

[12] Na, T. Y. & Habib, I. S. Solution of the natural convection problem by parameter differentiation. *Int. J. Heat Mass Transfer* **17**, 457–459 (1974).

[13] Merkin, J. H. A note on the similarity solutions for free convection on a vertical plate. *J. Engng. Math.* **19**, 189–201 (1985).

[14] Merkin, J. H. & Pop, I. Conjugate free convection on a vertical surface. *Int. J. Heat Mass Transfer* **39**, 1527–1534 (1996).

[15] Ali, F. M., Nazar, R. & Arifin, M. Numerical investigation of free convective boundary layer in a viscous fluid. *The American Journal of Scientific Research* **5**, 13–19 (2009).

[16] Motsa, S. S., Shateyi, S. & Makukula, Z. Homotopy analysis of free convection boundary layer flow with heat and mass transfer. *Chemical Engineering Communications* **198**, 783–795 (2011).

[17] Motsa, S. S., Makukula, Z. G. & Shateyi, S. Spectral Local Linearisation Approach for Natural Convection Boundary Layer Flow. *Hindawi Publishing Corporation Mathematical Problems in Engineering* **2013**, Article ID 765013, 7 pages (2013).

[18] Ghotbi, A. R. Bararnia, H., Domairry, G. & Barari, A. Investigation of a powerful analytical method into natural convection boundary layer flow. *Communications in Nonlinear Science and Numerical Simulation* **14(5)**, 2222–2228 (2009).

[19] Sobamowo, M. G. & Yinusa, A. A. Insight into the Boundary Layer Flows of Free Convection and Heat Transfer of Nanofluids Over a Vertical Plate using Multi-Step Differential Transformation Method. *Iranian Journal of Mechanical Engineering* **20(1)**, 1–42 (2019).